

Notes

Syntheses of Metallomacrocycles Containing Metal Amide Linkages. The X-ray Crystal Structure of *syn*-[Mo(NO)[HB(3,5-Me₂C₃HN₂)₃]{(4-NHC₆H₄)₂CO}]₂

Helen A. Jones, Thomas A. Hamor,
Christopher J. Jones,* Ferida S. McQuillan,
Keith Paxton, and Natalie M. Rowley

School of Chemistry, University of Birmingham, Edgbaston,
Birmingham B15 2TT, U.K.

Received July 7, 2000

Introduction

Cyclophane-like binuclear metallomacrocycles can be constructed in simple one-step reactions involving a suitable mononuclear metal complex precursor and a suitable ditopic proligand (Figure 1).^{1–3} Some reported examples contain {Pd(H₂NCH₂CH₂NH₂)₂}²⁺ and pyridyl ligands,⁴ {Zr(η⁵-C₅H₅)₂}²⁺ and alkoxy ligands,⁵ or {Mo(NO)(Tp^{Me2})₂}²⁺ {Tp^{Me2} = HB(3,5-Me₂C₃HN₂)₃} and ligands E–A–E (E = O, S; A = hydrocarbon-diyl).^{6–9} Since it is known¹⁰ that bis-organoamide derivatives [Mo(NO)(Tp^{Me2})(NHR)₂] (R = alkyl or aryl) can be formed from [Mo(NO)(Tp^{Me2})₂], we have investigated the possibility of synthesizing metallomacrocycles through the formation of molybdenum–amide bonds in direct reactions between [Mo(NO)(Tp^{Me2})₂] and ditopic diamine ligands. The new compounds **1–4** were obtained from these reactions (Figure 2).

Experimental Section

All commercial reagents were used as supplied unless otherwise stated. The complex [Mo(NO)(Tp^{Me2})₂]₂·C₆H₅Me¹¹ was prepared by a previously reported method. Solvents used as reaction media were dried and freed of oxygen before use by standard methods. Reactions were carried out under a dinitrogen atmosphere, but products were purified in air. Merck aluminum oxide (90) was used as the stationary phase for column chromatography. Infrared spectra were recorded as KBr pellets using a Perkin-Elmer 1600 series FT-IR spectrophotometer. The 300 MHz ¹H NMR spectra were measured using a Bruker AC 300 spectrometer, and liquid secondary ion mass spectra (LSIMS) were measured using a VG ZABSPEC mass spectrometer. Cyclic voltam-

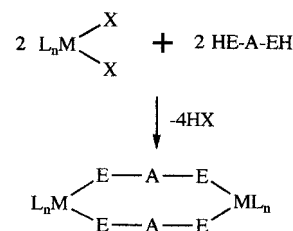
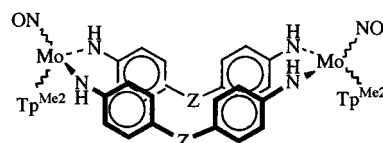


Figure 1. Examples of the formation of binuclear metallomacrocycles [ML_n(EAE)]₂, where L_nM = {(NH₂CH₂CH₂NH₂)Pd}²⁺ and E–A–E = 1,4-(NC₅H₄)₂C₆F₄;¹ L_nM = {Zr(η⁵-C₅H₅)₂} and EAE = 1,3-(OCH₂)₂C₆H₄;⁵ L_nM = {Mo[HB(3,5-Me₂C₃HN₂)₃](NO)} and EAE = 2,7-O₂C₁₀H₆; 1, *x*-(SCH₂)₂C₆H₄, *x* = 3,4; 4,4'-(OC₆H₄)₂CH₂.^{6–9}



- 1a:** Z = CH₂ *anti*-isomer
1s: Z = CH₂ *syn* isomer
2: Z = CH₂CH₂
3: Z = CO *syn* isomer

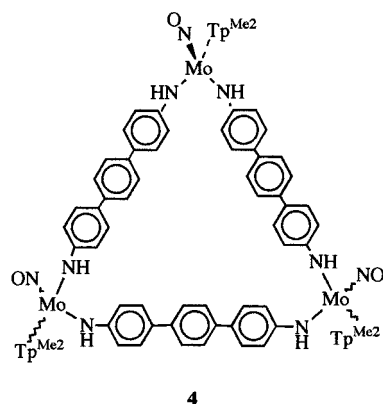


Figure 2. Structural formulas for compounds **1–4**.

metry was carried out using an EG&G model 362 potentiostat and the Condecon 310 hardware/software package. Measurements were made using approximately 2 × 10⁻³ mol dm⁻³ solutions in dry dichloromethane under an atmosphere of nitrogen. A 0.2 mol dm⁻³ solution of [Bu₄N][BF₄] was used as the base electrolyte. A platinum bead electrode was used, and potentials were measured with reference to ferrocene, which was used as an internal standard. UV/vis spectra were obtained using a Perkin-Elmer λ3 spectrophotometer. Elemental analyses were carried out at the microanalytical laboratories, University of North London.

syn- and anti-[Mo(NO)(Tp^{Me2}){(4-NHC₆H₄)₂CH₂}]₂ (1s and 1a). A solution of [Mo(NO)(Tp^{Me2})₂]₂·C₆H₅Me (1.00 g, 1.3 mmol) and (4-NH₂C₆H₄)₂CH₂ (0.292 g, 1.5 mmol) in dry toluene (50 cm³) containing Na (0.1 g, excess) was heated under reflux, with stirring for 18 h. The product mixture was then allowed to cool before being filtered to remove any unreacted Na. The solvent was removed in vacuo and the products separated by column chromatography using dichloromethane/hexane (1:1) as the eluant.

1a. *anti*-[Mo(NO)(Tp^{Me2}){(4-NHC₆H₄)₂CH₂}]₂ (yield 12%). ¹H NMR (300 MHz, CDCl₃, 293 K): δ 8.83 (4H, s, NH), 7.19, 6.95 (8H, d, J_{HH}

- (1) Fujita, M.; Ogura, K. *Bull. Chem. Soc. Jpn.* **1996**, *69*, 1471–1482.
 (2) Leininger, S.; Stang, P. J.; Olenyuk, B. *Chem. Rev.* **2000**, *100*, 853–907.
 (3) Jones, C. J. *Chem. Soc. Rev.* **1998**, *27*, 289–301.
 (4) Fujita, M.; Nagao, S.; Iida, M.; Ogata, K.; Ogura, K. *J. Am. Chem. Soc.* **1993**, *115*, 1574–1576.
 (5) Stephan, D. W. *Organometallics* **1990**, *9*, 2718–2723.
 (6) McQuillan, F. S.; Chen, H.; Hamor, T. A.; Jones, C. J.; Paxton, K. *Inorg. Chem.* **1997**, *36*, 4458–4464.
 (7) Hinton, H. A.; Chen, H.; Hamor, T. A.; Jones, C. J.; McQuillan, F. S.; Tolley, M. S. *Inorg. Chem.* **1998**, *37*, 2933–2942.
 (8) McQuillan, F. S.; Berridge, T. E.; Chen, H.; Hamor, T. A.; Jones, C. J. *Inorg. Chem.* **1998**, *37*, 4959–4970.
 (9) McQuillan, F. S.; Chen, H.; Hamor, T. A.; Jones, C. J.; Jones, H. A.; Sidebotham, R. P. *Inorg. Chem.* **1999**, *38*, 1555–1562.
 (10) Obaidi, N. A.; Hamor, T. A.; Jones, C. J.; McCleverty, J. A.; Paxton, K. *J. Chem. Soc., Dalton Trans.* **1986**, 1525–1530.
 (11) Reynolds, S. J.; Smith, C. F.; Jones, C. J.; McCleverty, J. A.; Bower, D. C.; Templeton, J. L. *Inorg. Synth.* **1985**, *23*, 4–9.

= 8 Hz, 8H, d, $J_{\text{HH}} = 8$ Hz; 4-(C₆H₄)₂, 5.95, 5.74 (2H, s, 4H, s; (CH₃)₂C₃N₂H-4), 3.86 (4H, s; 4-CH₂), 2.46, 2.44, 2.35, 2.34 (6H, s, 6H, s, 12H, s, 12H, s; 3,5-(CH₃)₂C₃N₂H). (+)-FABMS: m/z 1239 (M⁺). Anal. Found: C, 54.5; H, 5.6; N, 20.3. Calcd for *anti*-C₅₆H₆₈N₁₈O₂B₂Mo₂: C, 54.3; H, 5.5; N, 20.3. IR data (KBr disk): 3306 (ν_{NH}), 2545 (ν_{BH}), 1624 (ν_{NO}) cm⁻¹.

1s. *syn*-[Mo(NO)(Tp^{Me2}){4-(NHC₆H₄)₂CH₂}]₂ (yield 8%). ¹H NMR (300 MHz, CDCl₃, 293 K): δ 8.69 (4H, s; NH), 7.16 (16H, s; 4-(C₆H₄)₂), 5.88, 5.76 (2H, s, 4H, s; (CH₃)₂C₃N₂H-4), 3.92, 3.47 (2H, d, $J_{\text{HH}} = 13$ Hz, 2H, d, $J_{\text{HH}} = 13$ Hz; 4-CH₂), 2.43, 2.41, 2.34, 2.23 (6H, s, 12H, s, 12H, s, 6H, s; 3,5-(CH₃)₂C₃N₂H). (+)-FABMS: m/z 1239 (M⁺). Anal. Found: C, 54.0; H, 5.4; N, 20.3. Calcd for *syn*-C₅₆H₆₈N₁₈O₂B₂Mo₂: C, 54.3; H, 5.5; N, 20.3. IR data (KBr disk): 3318 (ν_{NH}), 2544 (ν_{BH}), 1636 (ν_{NO}) cm⁻¹.

[Mo(NO)(Tp^{Me2}){1,2-(4'-NHC₆H₄)₂C₂H₄}]₂ (**2**). This compound was prepared according to the preceding procedure using 1,2-(4'-NH₂C₆H₄)₂C₂H₄ (0.32 g, 1.5 mmol). The product was separated by column chromatography using dichloromethane/hexane (6:4) as the eluant (yield, 15%). ¹H NMR (300 MHz, CDCl₃, 293 K): δ 8.70 (4H, s; NH), 7.08 (16H, s; 4-(C₆H₄)₂), 5.87, 5.70 (2H, s, 4H, s; (CH₃)₂C₃N₂H-4), 3.17, 3.04 (4H, m, 4H, m; C₂H₄), 2.43, 2.32, 2.25 (6H, s, 12H, s, 18H, s; 3,5-(CH₃)₂C₃N₂H). (+)-FABMS: m/z 1268 (M⁺). Anal. Found: C, 54.7; H, 5.7; N, 19.7. Calcd for C₅₈H₇₂N₁₈O₂B₂Mo₂: C, 54.9; H, 5.7; N, 19.9. IR data (KBr disk): 3314 (ν_{NH}), 2532 (ν_{BH}), 1631 (ν_{NO}) cm⁻¹.

[Mo(NO)(Tp^{Me2}){4-(NHC₆H₄)₂CO}]₂ (**3**). This compound was prepared following the procedure described for **2**, using (4-NH₂C₆H₄)₂CO (0.313 g, 1.5 mmol). The product was separated by column chromatography using dichloromethane/hexane (6:4) as the eluant (yield, 3%). ¹H NMR (300 MHz, CDCl₃, 293 K): δ 8.96 (4H, s, NH), 7.95, 7.31 (8H, d, $J_{\text{HH}} = 8$ Hz, 8H, d, $J_{\text{HH}} = 8$ Hz; 4-(C₆H₄)₂), 5.93, 5.85 (2H, s, 4H, s; (CH₃)₂C₃N₂H-4), 2.48, 2.46, 2.39, 2.23 (12H, s, 6H, s, 12H, s, 6H, s; 3,5-(CH₃)₂C₃N₂H). ¹H NMR (300 MHz, {(CD₃)₂CO, 293 K}: δ 9.73 (4H, s, NH), 7.95, 7.58 (8H, d, $J_{\text{HH}} = 8$ Hz, 8H, d, $J_{\text{HH}} = 8$ Hz; 4-(C₆H₄)₂), 6.01, 5.97 (2H, s, 4H, s; (CH₃)₂C₃N₂H-4), 2.53, 2.49, 2.45, 2.27 (6H, s, 12H, s, 12H, s, 6H, s; 3,5-(CH₃)₂C₃N₂H). (+)-FABMS: m/z 1268 (M⁺). Anal. Found: C, 53.2; H, 5.2; N, 20.0. Calcd for C₅₆H₆₄N₁₈O₄B₂Mo₂: C, 53.1; H, 5.1; N, 19.9. IR data (KBr disk): 3302 (ν_{NH}), 2542 (ν_{BH}), 1640 (ν_{NO}) cm⁻¹.

[Mo(NO)(Tp^{Me2}){1,4-(4'-NHC₆H₄)₂C₆H₄}]₃ (**4**). This compound was prepared following the procedure described for **3** using 1,4-(4'-NH₂C₆H₄)₂C₆H₄ (0.384 g, 1.5 mmol). The product was separated by column chromatography using dichloromethane/hexane (1:1) as the eluant (yield, 2%). ¹H NMR (300 MHz, CDCl₃, 293 K): δ 8.90 (6H, s, NH), 7.52 (36H, m; 4,4'-(C₆H₄)₃), 5.96, 5.79 (3H, s, 6H, s; (CH₃)₂C₃N₂H-4), 2.48, 2.41, 2.36 (9H, s, 18H, s, 27H, m; 3,5-(CH₃)₂C₃N₂H). (+)-FABMS: m/z 2044 (M⁺). Anal. Found: C, 58.1; H, 5.4; N, 18.7. Calcd for C₉₉H₁₀₈N₂₇O₃B₃Mo₃: C, 58.1; H, 5.3; N, 18.5. IR data (KBr disk): 3310 (ν_{NH}), 2542 (ν_{BH}), 1642 (ν_{NO}) cm⁻¹.

Structural Studies. Crystals of complex **3** were grown by slow evaporation of a solution in a CH₂Cl₂/hexane mixture. Cell dimensions and intensity data for **3** were measured on a Rigaku R-Axis II area detector diffractometer (Table 1). The structure was determined¹² by direct methods and refined¹³ by least-squares on F^2 using anisotropic thermal parameters for non-hydrogen atoms, apart from the oxygen atoms of five putative water molecules, distributed over 13 partially occupied sites, which were refined with isotropic thermal parameters. Hydrogen atoms were placed in calculated positions, but those of the water molecules and a disordered dichloromethane were omitted. Figure 3 was drawn with ORTEP,¹⁴ thermal ellipsoids are at the 30% probability level.

Results and Discussion

Syntheses and Spectra. Initial attempts to synthesize metallomacrocycles from the ditopic diaminoaryl compounds H₂N-

Table 1. Crystallographic Data

formula	C ₅₆ H ₆₄ B ₂ N ₁₈ O ₄ Mo ₂ ·0.5CH ₂ Cl ₂ ·5H ₂ O
fw	1399.3
<i>a</i> , Å	17.075(2)
<i>b</i> , Å	21.067(3)
<i>c</i> , Å	21.429(3)
β , deg	97.45(2)
<i>V</i> , Å ³	7643(2)
<i>Z</i>	4
temp, °C	21
λ , Å	0.7107
space group	<i>P</i> 2 ₁ / <i>c</i>
ρ^{calcd}	1.216
μ (Mo K α), mm ⁻¹	0.420
$R_w(F_o^2)^a$	0.2051
$R(F_o)$ for obsd rflns ^b	0.0649
unique reflns	9137
obsvd rflns [$I > 2\sigma(I)$]	7630
largest diff peak, e Å ⁻³	0.79
largest diff hole, e Å ⁻³	-0.51

$$^a R_w(F_o^2) = [\sum w(F_o^2 - F_c^2)^2 / \sum w(F_o^2)^2]^{1/2}. \quad ^b R(F_o) = \sum (|F_o - F_c|) / \sum |F_o|.$$

A-NH₂ [A = 1,3- or 1,4-C₆H₄; 1,5- or 1,8-C₁₀H₆; (4-C₆H₄)₂Z, Z = CO, CH₂, CH₂CH₂; 1,3- or 1,4-(CH₂)₂C₆H₄; 1,4-(4'-C₆H₄)₂C₆H₄] and [Mo(NO)(Tp^{Me2})I₂] used the reaction conditions previously found to afford molybdenum bis-organoamide derivatives.^{12,13} However, neither these reaction conditions nor stepwise reactions involving the acyclic binuclear complexes {[Mo(NO)(Tp^{Me2})I]₂(HN-A-NH)} and further H₂N-A-NH₂ were found to produce metallomacrocycles. It did prove possible to produce metallomacrocycles when reactions were carried out in the presence of sodium metal, but only from certain diaryldiamines. The yields obtained were poor, and no macrocyclic products could be isolated from similar reactions involving proligands with alkylamine termini. Thus, the reactions carried out with (4-NH₂C₆H₄)₂CH₂, 1,2-(4'-NH₂C₆H₄)₂C₂H₄, or (4-NH₂C₆H₄)₂CO afforded the binuclear metallomacrocycles **1**, **2**, and **3**, respectively (Figure 2), whereas with 1,4-(4'-NH₂C₆H₄)₂C₆H₄ a trinuclear macrocycle **4** was obtained. In the case of **1** two isomers **1a** and **1s** could be separated by column chromatography, but in the cases of **2** and **3** only single isomers were isolated. The new metallomacrocycles were characterized by IR spectroscopy [$\nu_{\text{max}}(\text{BH})$ at ca. 2550; $\nu_{\text{max}}(\text{NH})$ in the region 3302–3318; $\nu_{\text{max}}(\text{NO})$ in the region 1624–1642 cm⁻¹], by ¹H NMR spectroscopy, and by (+)-LSIMS spectra, which contain molecular ions at the appropriate m/z values. An X-ray crystal structure determination (vide infra) was carried out on **3** and shows it to be the *syn* isomer.

The ¹H NMR spectra of the new compounds contained signals in the region to 5.7–6.0 ppm attributable to the pyrazolyl C⁴ protons. In the cases of **1a**, **1s**, **2**, and **3** these appeared as two signals in the area ratio 2:4 in accord with the presence of a plane of symmetry bisecting the Tp^{Me2} ligands. The pyrazolyl 3,5-methyl groups give rise to signals in the region 2.2–2.5 ppm in the area ratio 6:6:12:12. The amide protons appear as a broad singlet in the region 8.7–9.0 ppm. In addition signals due to the aryl and, in **1** and **2**, the methylene groups of the aryl amide ligands are present. The isomeric structures of **1a** and **1s** can be established from their ¹H NMR spectra because in the *anti* isomer (**1a**), the methylene protons of the bridging ligand are equivalent and appear as a singlet. In the case of the *syn* isomer (**1s**) the methylene protons comprise an AB system giving rise to two doublets (²*J* = 13 Hz).

The ¹H NMR spectrum of the trimer **4** contains signals in the area ratio 6:3 and 9:18:27 for the pyrazolyl C⁴ and 3,5-Me protons, respectively, consistent with the presence of a plane

(12) *TeXsan: Single Crystal Analysis Software*, version 1.6; Molecular Structure Corporation: The Woodlands, TX, 1993.

(13) Sheldrick, G. M. *SHELXL-93, Program for Crystal Structure Refinement*; University of Göttingen: Göttingen, Germany, 1993.

(14) Johnson, C. K. *ORTEP*; Report ORNL-5138; Oak Ridge National Laboratory: Oak Ridge, TN, 1976.

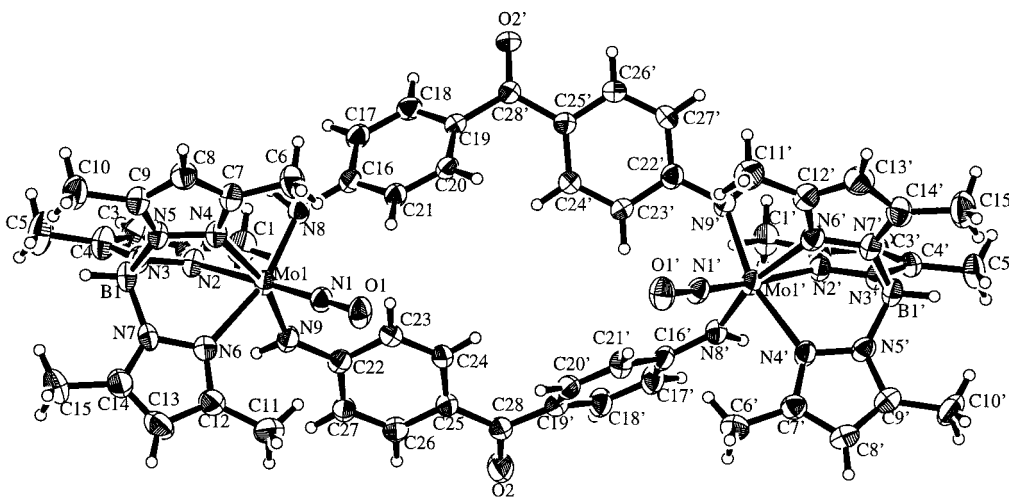


Figure 3. View of complex **3**. Primed atoms are related to the corresponding unprimed atoms by an approximate (noncrystallographic) 2-fold axis.

Table 2. Electronic Spectra and Electrochemical Data

complex	λ_{\max}^a (nm)	ϵ^a (mol ⁻¹ dm ³ cm ⁻¹)	E_f^b (V)	ΔE_p^c (mV)	i_{ap}/i_{cp}^d
1a	230	44 700	-1.94	210	0.9
	284	39 600			
	392	25 400			
1s	229	90 500	-1.90	190	0.9
	280	78 200			
	385	47 500			
2	228	55 100	-2.01	180	1.0
	276	27 300			
	376	42 800			
3	230	79 700	-1.39	75	0.8
	276	42 800			
	366	84 200			
4	228	59 900	-1.76	160	1.1
	336	63 700			

^a Recorded from solutions ca. 3×10^{-5} mol dm⁻³ in CH₂Cl₂.

^b Reduction potential referenced to ferrocene, measured from 10^{-3} mol dm⁻³ solutions of *complex* in CH₂Cl₂ containing 0.2 mol dm⁻³ [NBu₄][BF₄] as base electrolyte. Under these conditions the redox potential for the ferrocene/ferrocenium couple used as an internal standard was 0.545 ± 0.005 V vs SCE with ΔE_p in the range 75 ± 10 mV. ^c Difference in potential between the anodic and cathodic peaks of the cyclic voltammogram. ^d Ratio of anodic to cathodic peak current.

of symmetry bisecting each {Mo(NO)(Tp^{Me2})₂}²⁺ fragment. In [Mo(NO)(Tp^{Me2})(1,4-O₂C₆H₄)₃] this pattern has been observed for the syn,syn isomer.^{8c} However, in the case of **4** the {Mo(NO)(Tp^{Me2})₂} groups are separated by a much larger distance so that the Tp^{Me2} proton resonances may no longer be significantly affected by the orientation of the neighboring {Mo(NO)(Tp^{Me2})₂} groups. Thus, it is not possible to be certain that this compound has been isolated as a single isomer rather than a mixture of isomers. Crystals of **4** suitable for an X-ray diffraction study could not be obtained.

The electronic spectra (Table 2) of the new compounds all show absorptions at about 230 nm attributable to Tp^{Me2} π - π^* transitions. In addition **1a**, **1s**, **2**, and **3** contain absorptions at about 280 nm, which can be attributed to nitrosyl to metal charge transfer (LMCT), and absorptions at about 380 nm, which may be due to amide ligand to Mo LMCT.¹¹ In **4** only one band is observed in this region at 336 nm. This could result from the lower energy of the filled π orbitals of the triaryl group, giving a higher energy LMCT band that overlaps the NO to Mo LMCT to give a single broad absorption.

Electrochemical Studies. The reduction potentials of the new complexes were obtained from dichloromethane solutions by

cyclic voltammetry, and the results are presented in Table 2. In general, the values are in accord with expectations based on results reported previously for acyclic arylamide complexes of this type.^{10,15} The complexes **1a**, **1s**, **2**, and **4** undergo a single broad chemically reversible reduction process at a potential of ca. -1.75 V (vs ferrocene/ferrocenium). This is consistent with the presence of weakly interacting redox centers.¹⁶ However, in the case of **3** the carbonyl group linking the two aryl amide moieties allows a small interaction between the redox centers. Hence, two reduction waves are resolved in the first derivative of the cyclic voltammogram at potentials separated by 160 mV, corresponding to a comproportionation constant (K_c) of about 500. This value is somewhat larger than those found for similar acyclic binuclear complexes [Mo(NO)(Tp^{Me2})X]₂{(4-EC₆H₄)₂Z}]₂ (X = I, E = NH, Z = CH₂, K_c = 11; X = I, E = NH, Z = CH₂CH₂, K_c = 6; X = I, E = NH, Z = O, K_c = 76; X = I, E = NH, Z = SO₂, K_c = 191; X = Cl, E = O, Z = CO, K_c = 27).¹⁶ A comparison of the E_f values for the two isomers **1a** and **1s** reveals a small difference between the syn and anti forms. This is just significant to allow for errors of up to ± 10 mV in the measurement of E_f , and similar small differences have been found⁷ between the reduction potentials of the syn and anti isomers of [Mo(NO)(Tp^{Me2}){1,*x*-(SCH₂)₂C₆H₄}]₂ (ca. 30 mV for x = 3, ca. 60 mV for x = 4).

Structural Studies. A view of complex **3** is shown in Figure 1, and selected geometric parameters are listed in Table 3. The complex has no crystallographic symmetry but exhibits an approximate 2-fold (C_2) axis of symmetry. The coordination geometry at the molybdenum atoms is approximately octahedral in each case. Mean deviations from ideal octahedral are 6.8° at Mo(1) and 7.0° at Mo(1'). As had been noted previously,^{6,9} these deviations show a consistent pattern and differences between corresponding angles at the two molybdenum centers are relatively small, the mean difference being 0.6°. Comparison of these molybdenum centers with monomeric^{17,18} and other binuclear^{6,9} {Mo(NO)(Tp^{Me2})₂}²⁺-containing complexes shows

- (15) AlObaidi, N.; Chaudhury, M.; Clague, D.; Jones, C. J.; Pearson, J. C.; McCleverty, J. A.; Salam, S. S. *J. Chem. Soc., Dalton Trans.* **1987**, 1733-1736.
 (16) Charsley, S. M.; Jones, C. J.; McCleverty, J. A.; Neaves, B. D.; Reynolds, S. J. *J. Chem. Soc., Dalton Trans.* **1988**, 301-307.
 (17) AlObaidi, N.; Hamor, T. A.; Jones, C. J.; McCleverty, J. A.; Paxton, K. *J. Chem. Soc., Dalton Trans.* **1987**, 1063-1069.
 (18) Coe, B. J.; Hamor, T. A.; Jones, C. J.; McCleverty, J. A.; Bloor, D.; Cross, G. H.; Axon, T. L. *J. Chem. Soc., Dalton Trans.* **1995**, 673-684.

Table 3. Selected Structural Parameters^a

		Distances (Å)	
Mo(1)–N(1)	1.748(6)	Mo(1')–N(1')	1.770(6)
Mo(1)–N(2)	2.239(5)	Mo(1')–N(2')	2.246(5)
Mo(1)–N(4)	2.209(5)	Mo(1')–N(4')	2.202(6)
Mo(1)–N(6)	2.227(6)	Mo(1')–N(6')	2.233(6)
Mo(1)–N(8)	1.991(5)	Mo(1')–N(8')	1.987(6)
Mo(1)–N(9)	2.023(6)	Mo(1')–N(9')	2.023(5)
O(1)–N(1)	1.214(7)	O(1')–N(1')	1.195(7)
N(8)–C(16)	1.390(8)	N(8')–C(16')	1.397(8)
N(9)–C(22)	1.378(8)	N(9')–C(22')	1.383(8)
		Angles (deg)	
N(1)–Mo(1)–N(2)	178.4(2)	N(1')–Mo(1')–N(2')	177.6(2)
N(1)–Mo(1)–N(4)	95.2(2)	N(1')–Mo(1')–N(4')	95.8(2)
N(1)–Mo(1)–N(6)	96.3(2)	N(1')–Mo(1')–N(6')	94.6(2)
N(1)–Mo(1)–N(8)	96.1(2)	N(1')–Mo(1')–N(8')	96.9(2)
N(1)–Mo(1)–N(9)	94.0(2)	N(1')–Mo(1')–N(9')	94.0(2)
N(2)–Mo(1)–N(4)	86.2(2)	N(2')–Mo(1')–N(4')	85.5(2)
N(2)–Mo(1)–N(6)	83.4(2)	N(2')–Mo(1')–N(6')	83.7(2)
N(2)–Mo(1)–N(8)	84.5(2)	N(2')–Mo(1')–N(8')	85.0(2)
N(2)–Mo(1)–N(9)	84.4(2)	N(2')–Mo(1')–N(9')	84.2(2)
N(4)–Mo(1)–N(6)	78.7(2)	N(4')–Mo(1')–N(6')	78.4(2)
N(4)–Mo(1)–N(8)	91.5(2)	N(4')–Mo(1')–N(8')	90.6(2)
N(4)–Mo(1)–N(9)	163.9(2)	N(4')–Mo(1')–N(9')	162.7(2)
N(6)–Mo(1)–N(8)	164.9(2)	N(6')–Mo(1')–N(8')	164.8(2)
N(6)–Mo(1)–N(9)	87.3(2)	N(6')–Mo(1')–N(9')	86.7(2)
N(8)–Mo(1)–N(9)	100.5(2)	N(8')–Mo(1')–N(9')	102.3(2)
O(1)–N(1)–Mo(1)	178.7(5)	O(1')–N(1')–Mo(1')	177.0(6)
C(16)–N(8)–Mo(1)	141.1(4)	C(16')–N(8')–Mo(1')	139.2(5)
C(22)–N(9)–Mo(1)	134.3(5)	C(22')–N(9')–Mo(1')	133.2(5)
		Torsion Angles (deg)	
N(1)–Mo(1)–N(8)–C(16)	10.1(7)	N(1')–Mo(1')–N(8')–C(16')	13.0(7)
N(1)–Mo(1)–N(9)–C(22)	–28.9(6)	N(1')–Mo(1')–N(9')–C(22')	–25.8(7)

^a Values in parentheses are estimated standard deviations.

that the mean differences between corresponding angles are of similar magnitude.

The C(phenyl)–N–Mo angles are large, 133.2–141.1°, and the corresponding Mo–N bonds are short. This implies p_{π} – d_{π} electron donation from the donor atom (N) to the coordinatively unsaturated metal. The small N(nitrosyl)–Mo–N–C(phenyl) torsion angles (less than $\pm 28.9^\circ$) are consistent with this, although steric effects may also play a role in increasing the bond angle at nitrogen. It is noteworthy that the larger bond angles at N(8) and N(8'), the mean being 140.1°, are associated with the smaller N(nitrosyl)–Mo–N–C(phenyl) torsion angles, the mean being 11.5° (see Table 3). The phenyl rings are fairly close to coplanarity with their respective Mo–N–C planes (dihedral angles in the range 12.4–30.5°), and the N–C(phenyl) bonds are relatively short (Table 3), suggesting¹⁷ some conjugation with the phenyl rings.

The capacity of cyclic complexes to bind guest molecules is governed by the size of the cavity formed. The O(1)···O(1') distance is 7.12(1) Å, so the nitrosyl ligands would not bar the central cavity to a potential guest molecule. The opposite, lower face is even more open (Figure 1), and the complex would appear to have the capacity to bind small guest molecules. Critical cross-ring interatomic distances are C(24)···C(24') 5.13 Å, C(23)···C(24') 5.55 Å, and C(24)···C(23') 5.53 Å. The corresponding H···H distances are approximately 3.48, 4.18, and 4.12 Å, respectively. However, although the crystal contains solvent of crystallization, a disordered dichloromethane molecule with approximately 50% site occupancy, together with some 13 partially occupied sites considered to represent water molecules, none of these is positioned within the central cavity of the complex. The only significant contact is between one of the water molecules and the nitrosyl oxygen atom, O(1'), of 3.18 Å, with an N–O···O(water) angle of 149°. A hydrogen

bond may be involved here, but the water molecule lies above the NO ligand outside the cavity. The dichloromethane and the other water molecules appear to act only as space fillers.

In crystals of *anti*-[Mo(NO)(Tp^{Me2}){1,4-(OCH₂)₂C₆H₄}]₂·4CHCl₃ the ligated oxygen atoms have been found to function as hydrogen bond acceptor sites toward hydrogen on two of the chloroform molecules.⁹ Since the presence of the amide donor group in the new compounds offers potential hydrogen bond donor sites, which might interact with hydrogen bond acceptor solvents, attempts were made to crystallize solvates of the new macrocycles with potential hydrogen bond acceptor solvents such as acetone. Unfortunately these attempts failed to produce crystalline solvates. It was found that the chemical shifts of the amide protons of **1a**, **1s**, and **2** were little affected by a change in solvent from CDCl₃ to (CD₃)₂CO; only in the case of **3** was a significant change in shift from 8.96 to 9.73 ppm observed. The other signals from **3** show much smaller differences in chemical shift, the largest being 0.27 ppm for one of the aryl proton signals. Thus, it seems that interactions with hydrogen bond acceptor solvents are weak. In the case of **3** the crystal structure shows no evidence of interactions between the amide hydrogen atoms and the solvent molecules in the solid state.

Conclusion

It seems that the chemistry of Mo–NH bond formation in these {Mo(NO)(Tp^{Me2})} derivatives is far less suited to metal-macrocycle formation than either Mo–O or Mo–S bond formation. The two major differences between the two types of ligand are the presence of the amide hydrogen, which may have some steric consequences, and the stronger electron-donor character of the amide group toward the metal center. This is evident in the reduction potentials of the arylamide complexes,

which are more negative than those of their aryloxy counterparts, by 580 mV for $[\text{Mo}(\text{NO})(\text{Tp}^{\text{Me}_2})(\text{EPh})_2]$ ($\text{E} = \text{O}, \text{NH}$).¹⁵ It may be that this has a labilizing effect on the Mo–N(amide) bonds, leading to poorer yields of metallomacrocycles formed in kinetic processes.

Acknowledgment. We are grateful to Mr. M. Tolley and Mr. P. R. Ashton for spectroscopic measurements. We thank the EPSRC and the University of Birmingham for funds to purchase the R-Axis II diffractometer, and we also thank the

Leverhulme Trust and the EPSRC (Grants GR/J87572 and GR/M14234) for supporting this work.

Supporting Information Available: X-ray crystallographic files in CIF format for the structure determination of *syn*- $\{[\text{Mo}(\text{NO})[\text{HB}(3,5\text{-Me}_2\text{C}_3\text{HN}_2)_3]\{4\text{-NHC}_6\text{H}_4)_2\text{CO}\}_2$. This material is available free of charge via the Internet at <http://pubs.acs.org>.

IC000749A